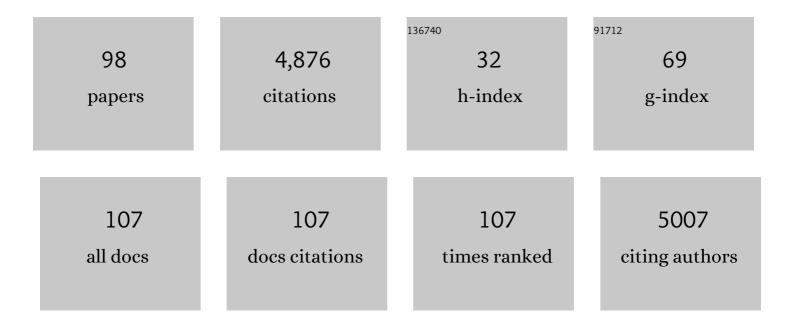
## Robert K Szilagyi

List of Publications by Year in descending order

Source: https://exaly.com/author-pdf/6852405/publications.pdf Version: 2024-02-01



#	Article	IF	CITATIONS
1	Electronic Structures of Metal Sites in Proteins and Models:Â Contributions to Function in Blue Copper Proteins. Chemical Reviews, 2004, 104, 419-458.	23.0	782
2	Ligand K-edge X-ray absorption spectroscopy: covalency of ligand–metal bonds. Coordination Chemistry Reviews, 2005, 249, 97-129.	9.5	326
3	Dithiomethylether as a Ligand in the Hydrogenase H-Cluster. Journal of the American Chemical Society, 2008, 130, 4533-4540.	6.6	304
4	A Mononuclear Fe(III) Single Molecule Magnet with a 3/2↔5/2 Spin Crossover. Journal of the American Chemical Society, 2012, 134, 13651-13661.	6.6	256
5	Spectroscopic Calibration of Modern Density Functional Methods Using [CuCl4]2 Journal of Physical Chemistry A, 2002, 106, 2994-3007.	1.1	195
6	Description of the Ground State Wave Functions of Ni Dithiolenes Using Sulfur K-edge X-ray Absorption Spectroscopy. Journal of the American Chemical Society, 2003, 125, 9158-9169.	6.6	180
7	Sulfur K-Edge X-ray Absorption Spectroscopy as a Probe of Ligandâ^'Metal Bond Covalency:Â Metal vs Ligand Oxidation in Copper and Nickel Dithiolene Complexes. Journal of the American Chemical Society, 2007, 129, 2316-2326.	6.6	168
8	A Quantitative Description of the Ground-State Wave Function of CuAby X-ray Absorption Spectroscopy:Â Comparison to Plastocyanin and Relevance to Electron Transfer. Journal of the American Chemical Society, 2001, 123, 5757-5767.	6.6	153
9	Structural, Spectroscopic, and Theoretical Elucidation of a Redox-Active Pincer-Type Ancillary Applied in Catalysis. Journal of the American Chemical Society, 2008, 130, 3676-3682.	6.6	144
10	The Solution Structure of [Cu(aq)]2+and Its Implications for Rack-Induced Bonding in Blue Copper Protein Active Sites. Inorganic Chemistry, 2005, 44, 1922-1933.	1.9	134
11	Structure and Bonding of the Isoelectronic Hexacarbonyls [Hf(CO)6]2-, [Ta(CO)6]-, W(CO)6, [Re(CO)6]+, [Os(CO)6]2+, and [Ir(CO)6]3+:  A Theoretical Study1. Organometallics, 1997, 16, 4807-4815.	1.1	128
12	Activation of HydA <sup>ΔEFG</sup> Requires a Preformed [4Fe-4S] Cluster. Biochemistry, 2009, 48, 6240-6248.	1.2	119
13	Exploring new frontiers of nitrogenase structure and mechanism. Current Opinion in Chemical Biology, 2006, 10, 101-108.	2.8	116
14	On the accuracy of density functional theory for iron—sulfur clusters. Journal of Computational Chemistry, 2006, 27, 1385-1397.	1.5	107
15	Three-Coordinate Copper(I) Amido and Aminyl Radical Complexes. Journal of the American Chemical Society, 2009, 131, 3878-3880.	6.6	104
16	Probing the Electronic Structures of [Cu <sub>2</sub> (μ-XR <sub>2</sub> )] <i><sup>n</sup></i> <sup>+</sup> Diamond Cores as a Function of the Bridging X Atom (X = N or P) and Charge ( <i>n</i> = 0, 1, 2). Journal of the American Chemical Society, 2008, 130, 3478-3485.	6.6	87
17	Spectroscopic Investigation of Stellacyanin Mutants:Â Axial Ligand Interactions at the Blue Copper Site. Journal of the American Chemical Society, 2003, 125, 11314-11328.	6.6	85
18	Comparative Assessment of the Composition and Charge State of Nitrogenase FeMo-Cofactor. Inorganic Chemistry, 2011, 50, 4811-4824.	1.9	73

#	Article	IF	CITATIONS
19	S K-Edge X-ray Absorption Spectroscopic Investigation of the Ni-Containing Superoxide Dismutase Active Site:  New Structural Insight into the Mechanism. Journal of the American Chemical Society, 2004, 126, 3018-3019.	6.6	72
20	A radical solution for the biosynthesis of the H-cluster of hydrogenase. FEBS Letters, 2006, 580, 363-367.	1.3	72
21	Probing the role of the divalent metal ion in uteroferrin using metal ion replacement and a comparison to isostructural biomimetics. Journal of Biological Inorganic Chemistry, 2007, 13, 139-155.	1.1	59
22	Electronic Control of the "Bailar Twist―in Formally d <sup>0</sup> -d <sup>2</sup> Molybdenum Tris(dithiolene) Complexes: A Sulfur K-edge X-ray Absorption Spectroscopy and Density Functional Theory Study. Inorganic Chemistry, 2008, 47, 6382-6392.	1.9	57
23	Electronic structure and its relation to function in copper proteins. Current Opinion in Chemical Biology, 2002, 6, 250-258.	2.8	55
24	Spectroscopic Studies of the Met182Thr Mutant of Nitrite Reductase:Â Role of the Axial Ligand in the Geometric and Electronic Structure of Blue and Green Copper Sites. Journal of the American Chemical Society, 2003, 125, 14784-14792.	6.6	55
25	Theoretical Studies of Biological Nitrogen Fixation. I. Density Functional Modeling of the Mo-Site of the FeMo-Cofactor. Inorganic Chemistry, 2001, 40, 766-775.	1.9	46
26	Spectroscopic Characterization of the Leu513His Variant of Fungal Laccase:  Effect of Increased Axial Ligand Interaction on the Geometric and Electronic Structure of the Type 1 Cu Site. Inorganic Chemistry, 2003, 42, 4006-4017.	1.9	46
27	Sulfur K-Edge X-ray Absorption Spectroscopy and Density Functional Calculations on Mo(IV) and Mo(VI)â•O Bis-dithiolenes: Insights into the Mechanism of Oxo Transfer in DMSO Reductase and Related Functional Analogues. Journal of the American Chemical Society, 2010, 132, 8359-8371.	6.6	46
28	On the electronic structure of the hydrogenase H-cluster. Chemical Communications, 2006, , 3696.	2.2	44
29	Role of the Tyr-Cys Cross-link to the Active Site Properties of Galactose Oxidase. Inorganic Chemistry, 2012, 51, 3513-3524.	1.9	42
30	Can Steric Effects Induce the Mechanism Switch in the Rhodium-Catalyzed Imine Boration Reaction? A Density Functional and ONIOM Study. Organometallics, 2005, 24, 1938-1946.	1.1	34
31	Reduction of Nitrite and Nitrate to Ammonium on Pyrite. Origins of Life and Evolution of Biospheres, 2012, 42, 275-294.	0.8	34
32	Structure of the Oxidized Active Site of Galactose Oxidase from Realistic In Silico Models. Journal of the American Chemical Society, 2006, 128, 15550-15551.	6.6	33
33	Electronic structure of [Ni(II)S4] complexes from S K-edge X-ray absorption spectroscopy. Coordination Chemistry Reviews, 2013, 257, 564-578.	9.5	33
34	Influence of Ligand Flexibility on the Electronic Structure of Oxidized Ni <sup>III</sup> -Phenoxide Complexes. Inorganic Chemistry, 2014, 53, 10195-10202.	1.9	33
35	Theoretical studies of biological nitrogen fixation. Part II. Hydrogen bonded networks as possible reactant and product channels. Computational and Theoretical Chemistry, 2000, 506, 131-146.	1.5	29
36	Uranium Exerts Acute Toxicity by Binding to Pyrroloquinoline Quinone Cofactor. Environmental Science & Technology, 2011, 45, 937-942.	4.6	26

#	Article	IF	CITATIONS
37	Distorted tetrahedral nickel-nitrosyl complexes: spectroscopic characterization and electronic structure. Journal of Biological Inorganic Chemistry, 2016, 21, 757-775.	1.1	25
38	Sulfur K-edge XAS of WVO vs. MoVO bis(dithiolene) complexes: Contributions of relativistic effects to electronic structure and reactivity of tungsten enzymes. Journal of Inorganic Biochemistry, 2007, 101, 1594-1600.	1.5	24
39	Systematic development of computational models for the catalytic site in galactose oxidase: impact of outer-sphere residues on the geometric and electronic structures. Journal of Biological Inorganic Chemistry, 2008, 13, 371-383.	1.1	24
40	Iron–sulfur bond covalency from electronic structure calculations for classical iron–sulfur clusters. Journal of Computational Chemistry, 2014, 35, 540-552.	1.5	24
41	Insights into the role of nucleotide-dependent conformational change in nitrogenase catalysis: Structural characterization of the nitrogenase Fe protein Leu127 deletion variant with bound MgATP. Journal of Inorganic Biochemistry, 2006, 100, 1041-1052.	1.5	23
42	Protein environmental effects on ironâ€sulfur clusters: A set of rules for constructing computational models for inner and outer coordination spheres. Journal of Computational Chemistry, 2016, 37, 1681-1696.	1.5	23
43	Electronic structural investigations of ruthenium compounds and anticancer prodrugs. Journal of Biological Inorganic Chemistry, 2009, 14, 891-898.	1.1	22
44	Development of palladium L-edge X-ray absorption spectroscopy and its application for chloropalladium complexes. Inorganica Chimica Acta, 2008, 361, 1047-1058.	1.2	20
45	High Covalence in CuSO4and the Radicalization of Sulfate:Â An X-ray Absorption and Density Functional Study. Inorganic Chemistry, 2004, 43, 8318-8329.	1.9	18
46	Conversion of Carbon Dioxide to Oxalate by α-Ketocarboxylatocopper(II) Complexes. Inorganic Chemistry, 2014, 53, 8191-8193.	1.9	17
47	Thin-walled nanoscrolls by multi-step intercalation from tubular halloysite-10 Ã and its rearrangement upon peroxide treatment. Applied Surface Science, 2017, 399, 245-254.	3.1	16
48	Compositional and structural insights into the nature of the H-cluster precursor on HydF. Dalton Transactions, 2018, 47, 9521-9535.	1.6	16
49	Molecular Treatment of Nano-Kaolinite Generations. Inorganic Chemistry, 2018, 57, 7151-7167.	1.9	16
50	Electron and Spin Density Topology of the Hâ€Cluster and Its Biomimetic Complexes. European Journal of Inorganic Chemistry, 2011, 2011, 2677-2690.	1.0	14
51	A novel 1,3,5-triaminocyclohexane-based tripodal ligand forms a unique tetra(pyrazolate)-bridged tricopper( <scp>ii</scp> ) core: solution equilibrium, structure and catecholase activity. Dalton Transactions, 2016, 45, 14998-15012.	1.6	14
52	Surface Characterization of Mechanochemically Modified Exfoliated Halloysite Nanoscrolls. Langmuir, 2017, 33, 3534-3547.	1.6	14
53	Sulfur K-edge X-ray absorption spectroscopy as an experimental probe for S-nitroso proteins. Biochemical and Biophysical Research Communications, 2005, 330, 60-64.	1.0	13
54	Multi-edge X-ray Absorption Spectroscopy. 1. X-ray Absorption near-Edge Structure Analysis of a Biomimetic Model of FeFe-Hydrogenase, Journal of Physical Chemistry A, 2012, 116, 12280-12298	1.1	13

#	Article	IF	CITATIONS
55	Probing the MgATP-Bound Conformation of the Nitrogenase Fe Protein by Solution Small-Angle X-ray Scattering. Biochemistry, 2007, 46, 14058-14066.	1.2	12
56	Hydrogen Scrambling in [(C5Me5)Os(dmpm)(CH3)H]+. A Density Functional and ONIOM Study. Organometallics, 2002, 21, 555-564.	1.1	11
57	Electronic Structure of Transition Metalâ^'Cysteine Complexes from X-ray Absorption Spectroscopy. Journal of Physical Chemistry B, 2008, 112, 4770-4778.	1.2	11
58	The positions of inner hydroxide groups and aluminium ions in exfoliated kaolinite as indicators of the external chemical environment. Physical Chemistry Chemical Physics, 2014, 16, 25830-25839.	1.3	11
59	The origin of exo-selectivity in methyl cyanoformate addition onto the C bond of norbornene in Pd-catalyzed cyanoesterification. Dalton Transactions, 2014, 43, 9537-9548.	1.6	11
60	Radical S-adenosylmethionine maquette chemistry: Cx3Cx2C peptide coordinated redox active [4Fe–4S] clusters. Journal of Biological Inorganic Chemistry, 2019, 24, 793-807.	1.1	11
61	Reductive biomining of pyrite by methanogens. Trends in Microbiology, 2022, 30, 1072-1083.	3.5	10
62	Density functional studies of [(alkoxy-carbonyl)methyl]cobalt tricarbonyl triphenylphosphine complexes: an α-ester η3-coordination. Inorganica Chimica Acta, 2003, 344, 158-168.	1.2	9
63	Combined Mössbauer spectroscopic, multi-edge X-ray absorption spectroscopic, and density functional theoretical study of the radical SAM enzyme spore photoproduct lyase. Journal of Biological Inorganic Chemistry, 2014, 19, 465-483.	1.1	9
64	Behaviour of the surface hydroxide groups of exfoliated kaolinite in the gas phase and during water adsorption. Dalton Transactions, 2016, 45, 2523-2535.	1.6	9
65	The molecular mechanism of palladium-catalysed cyanoesterification of methyl cyanoformate onto norbornene. Dalton Transactions, 2016, 45, 7786-7793.	1.6	9
66	Kaolins of high iron-content as photocatalysts: Challenges of acidic surface modifications and mechanistic insights. Applied Clay Science, 2020, 195, 105722.	2.6	9
67	Production of a Biomimetic Fe <sup>(I)</sup> -S Phase on Pyrite by Atomic Hydrogen Beam Surface Reactive Scattering. Langmuir, 2011, 27, 6814-6821.	1.6	8
68	The Allosteric Regulation of Axial/Rhombic Population in a "Type 1―Copper Site: Multi-Edge X-ray Absorption Spectroscopic and Density Functional Studies of Pseudoazurin. Bulletin of the Chemical Society of Japan, 2015, 88, 1642-1652.	2.0	8
69	Multiedge X-ray Absorption Spectroscopy Part II: XANES Analysis of Bridging and Terminal Chlorides in Hexachlorodipalladate(II) Complex. Journal of Physical Chemistry A, 2015, 119, 5579-5586.	1.1	8
70	Secondary structure analysis of peptides with relevance to iron–sulfur cluster nesting. Journal of Computational Chemistry, 2019, 40, 515-526.	1.5	8
71	Molecular mechanical studies on the olefin metathesis reaction. Journal of Organometallic Chemistry, 1994, 465, 211-219.	0.8	7
72	Realistic molecular cluster models for exfoliated kaolinite. Clay Minerals, 2015, 50, 307-327.	0.2	7

#	Article	IF	CITATIONS
73	X-ray crystallographic evidence for the simultaneous presence of axial and rhombic sites in cupredoxins: atomic resolution X-ray crystal structure analysis of pseudoazurin and DFT modelling. RSC Advances, 2016, 6, 88358-88365.	1.7	7
74	Spin-Polarization-Induced Preedge Transitions in the Sulfur K-Edge XAS Spectra of Open-Shell Transition-Metal Sulfates: Spectroscopic Validation of Ï <i>f-</i> Bond Electron Transfer. Inorganic Chemistry, 2017, 56, 1080-1093.	1.9	7
75	Compositional, structural, and surface characterization of heat-treated halloysite samples: Influence of surface treatment on photochemical activity. Applied Clay Science, 2021, 212, 106222.	2.6	7
76	Molecular mechanics studies on the stereoselectivity of WCl6/SnMe4-catalyzed ring-opening polymerization of norbornene. Journal of Molecular Catalysis, 1992, 76, 145-156.	1.2	6
77	Electrochemically induced metal- <i>vs.</i> ligand-based redox changes in mackinawite: identification of a Fe <sup>3+</sup> - and polysulfide-containing intermediate. Dalton Transactions, 2021, 50, 11763-11774.	1.6	6
78	III. Modelling of the "well-defined―carbenes. Journal of Organometallic Chemistry, 1994, 475, 183-192.	0.8	5
79	Structure and reactivity of metathesis-active tungsta-carbenes. Journal of Organometallic Chemistry, 1995, 505, 81-83.	0.8	5
80	Evaluation of biosynthetic pathways for the unique dithiolate ligand of the FeFe hydrogenase H-cluster. Journal of Biological Inorganic Chemistry, 2010, 15, 1177-1182.	1.1	5
81	Nitrogenase Structure and Function Relationships by Density Functional Theory. Methods in Molecular Biology, 2011, 766, 267-291.	0.4	5
82	Natural selection based on coordination chemistry: computational assessment of [4Fe–4S]-maquettes with non-coded amino acids. Interface Focus, 2019, 9, 20190071.	1.5	5
83	Methane Adsorption on Heteroatom-Modified <i>Maquettes</i> of Porous Carbon Surfaces. Journal of Physical Chemistry A, 2021, 125, 6042-6058.	1.1	5
84	DTMM and COSMIC molecular mechanics parameters for alkylsilanes. Computational and Theoretical Chemistry, 1999, 490, 219-232.	1.5	4
85	Comparison of thallium(I) complexes with mesityl-substituted tris(pyrazolyl)hydroborate ligands, [Tl{HB(3-Ms-5-Mepz)3}] and [Tl{HB(3-Ms-5-Mepz)2(3-Me-5-Mspz)}]. Acta Crystallographica Section C, Structural Chemistry, 2016, 72, 786-790.	0.2	4
86	Mono- and binuclear tris(3- <i>tert</i> -butyl-2-sulfanylidene-1 <i>H</i> -imidazol-1-yl)hydroborate bismuth(III) dichloride complexes: a soft scorpionate ligand can coordinate to <i>p</i> -block elements. Acta Crystallographica Section C, Structural Chemistry, 2016, 72, 768-776.	0.2	4
87	Molecular mechanical studies on olefin metathesis reaction. Part 2: Modelling of {W[H2] (OCH2-t-Bu)2Br2}2 and W[H2] (OCH2-t-Bu)2Br2 ·GaBr3. Journal of Molecular Catalysis, 1994, 90, 157-170.	1.2	3
88	<i>In silico</i> evaluation of proposed biosynthetic pathways for the unique dithiolate ligand of the Hâ€cluster of [FeFe]â€hydrogenase. Journal of Computational Chemistry, 2011, 32, 3194-3206.	1.5	3
89	How Chemical Environment Activates Anthralin and Molecular Oxygen for Direct Reaction. Journal of Organic Chemistry, 2020, 85, 1315-1321.	1.7	2
90	dtmm/cosmic molecular mechanics parameters for alkylphosphines. Computational and Theoretical Chemistry, 1998, 427, 55-64.	1.5	1

#	Article	IF	CITATIONS
91	Initiation, Propagation and Termination of Olefin Metathesis Reactions. , 1998, , 157-187.		1
92	Non-innocent ground state electronic structure of a polynuclear copper complex with picolinate bridges. Inorganica Chimica Acta, 2018, 472, 307-319.	1.2	1
93	Evaluating Density Functionals by Examining Molecular Structures, Chemical Bonding, and Relative Energies of Mononuclear Ru–Cl–H–PR3 Isomers. Journal of Physical Chemistry A, 2019, 123, 343-358.	1.1	1
94	Electronic Structures of Metal Sites in Proteins and Models: Contributions to Function in Blue Copper Proteins. ChemInform, 2004, 35, no.	0.1	0
95	High Covalence in CuSO4 and the Radicalization of Sulfate: An X-Ray Absorption and Density Functional Study ChemInform, 2005, 36, no.	0.1	0
96	Meeting Report: XANES and EXAFS Spectroscopy of Materials and Biological Samples. Synchrotron Radiation News, 2006, 19, 14-15.	0.2	0
97	Ground electronic state description of thiourea coordination in homoleptic Zn <sup>2+</sup> , Ni <sup>2+</sup> and Co <sup>2+</sup> complexes using sulfur <i>K</i> -edge X-ray absorption spectroscopy. Journal of Synchrotron Radiation, 2021, 28, 1825-1838.	1.0	0
98	Molecular Mechanical Modeling of the Metathesis-Active Tungsta-Carbenes. , 1998, , 411-443.		0